https://doi.org/10.31896/k.29.6
Original scientific paper
Accepted: 10 November 2025

GEORG GLAESER

Geometric Construction of a Family of Keplerian Ellipses

A Geometric Construction of a Family of Keplerian Ellipses

ABSTRACT

We investigate a one-parameter family of Keplerian ellipses in a plane sharing a fixed focus F_1 and passing through a prescribed point P with identical instantaneous speed. By means of a purely geometric construction – the reflection of the ray F_1P in the tangent at P – the second focus F_2 is located on a circle f_2, yielding simple loci for the centers M and the secondary vertices C, D (both circles) and for the principal vertices A, B (conchoids of a circle). The family admits an envelope, itself an ellipse whose semiaxes are obtained in closed form. The configuration provides a direct geometric interpretation of the vis-viva relation: All members share the same semimajor axis a, and thus, the same orbital period. When rotated about the axis F_1P, the envelope ellipses form a family of confocal ellipsoids of revolution, thus connecting the planar Kepler construction with the classical geometry of quadrics.

Key words: Keplerian ellipses, envelope ellipse, conchoid, limaçon, vis-viva relation, energy equation

MSC2020: 70F15, 51A05, 51N20, 37J35

Geometrijska konstrukcija familije Keplerovih elipsa

SAŽETAK

Istražujemo jednoparametarsku familiju Keplerovih elipsa u ravnini koje imaju isto žarište F_1 i prolaze kroz danu točku P jednakom trenutnom brzinom. Pomoću čisto geometrijske konstrukcije – refleksija zrake F_1P na tangenti u točki P – drugo žarište F_2 leži na kružnici f_2, dobivaju se geometrijska mjesta središta M i sporednih tjemena C, D (dvije kružnice) i glavnih tjemena A, B (konhoide kružnice). Familija elipsi ima envelopu, također elipsu, čije su poluosi dobivene u zatvorenoj formi. Ova konfiguracija pruža izravno geometrijsko tumačenje vis-viva relacije: Svi članovi dijele istu veliku glavnu poluos a, pa onda i isti orbitni period. Kada rotiraju oko osi F_1P, elipse envelope tvore familiju konfokalnih rotacijskih elipsoida, čime se ravninska Keplerova konstrukcija povezuje s klasičnom geometrijom kvadrika.

Ključne riječi: Keplerove elipse, elipsa envelopa, konhoida, puž, vis-viva relacija, jednadžba energije

1 Motivation

This paper addresses certain physical relationships within the framework of Keplerian ellipses – not only from a physical but, above all, from a geometrical point of view – and arrives at several remarkable results. More specifically, it focuses on applying the vis-viva equation (energy equation of the Kepler orbit) to spatial objects, an approach that makes it possible to describe and analyse elliptical orbits in three-dimensional space in a fully consistent way (Fig. 1).

2 State of the Art and Related Work

The idea to organize Kepler orbits into families determined by position and speed goes back at least to Laporte [8], who studied the one-parameter family of ellipses obtained from a fixed point with equal initial speed and varying direction. Butikov provided an accessible modern account of such families and their qualitative geometry [2], and later discussed envelopes in the context of ballistic and elliptic trajectories [3]. Very recently, Heckman [7] revisited the family of Kepler ellipses through a fixed point from a geometric Hamiltonian viewpoint: He showed, in particular,

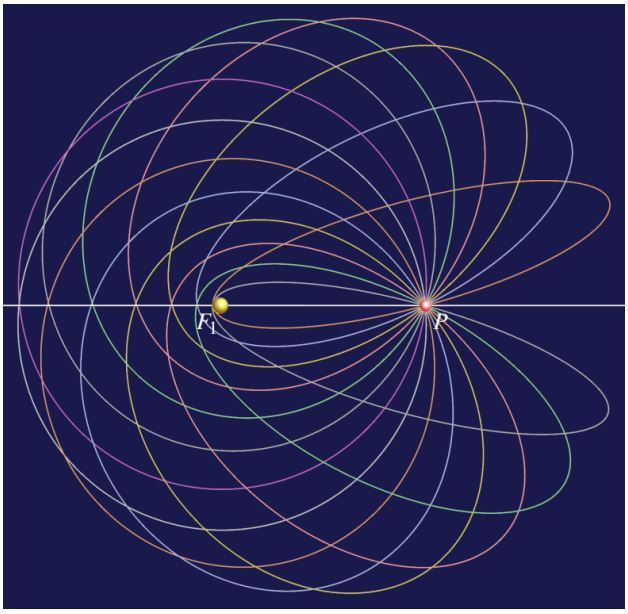

Figure 1: *Family of Keplerian ellipses corresponding to the same initial orbital speed* v*, but with different directions of the velocity vector* $\vec{v}$*. Each ellipse passes through the fixed point P and has the same focus* F_1.

that the locus of second foci is a circle of radius $2a - r$ centered at the passing point P, that all members share the same period, and he described a bounding ellipse for the swept region.

To the best of our knowledge, a *purely geometric* construction of the common *envelope ellipse* for the constant-speed family – based on reflecting the ray F_1P in the tangent at P and exploiting the collinearity of P, F_2 and the contact point – together with explicit *loci* for the centers (m), secondary vertices (C, D), and the conchoid loci for the major vertices (A, B), as well as the extremal configuration with maximal b and the cusped limaçon case $a = d$, does not appear explicitly in the literature cited above. The present paper provides such a unified geometric treatment and closed formulas for the envelope's semiaxes.

3 Introduction

Kepler's discovery that the planets move in ellipses rather than circles marks one of the most elegant links between geometry and physics. The corresponding vis-viva relation,

$$\mathrm{v}^2 = \mu\left(\frac{2}{r} - \frac{1}{a}\right),$$

connects the instantaneous distance r and speed v of a body in a central fields of gravitation with the global parameter a, the semimajor axis of its elliptical orbit.

We consider here, in purely geometric terms, the *family of all Keplerian ellipses* that share a fixed focus F_1 and pass through a given point P with identical speed. While the tangent direction in P varies, the energy and semimajor axis remain constant, forming a one-parameter family of ellipses. The central question is the determination of their *envelope*.

It is a matter of fact that the ray F_1P, when reflected in the tangent at P, passes through the second focus F_2 of the corresponding ellipse. The line PF_2 then meets the envelope in the point of contact, proving the collinearity of F_1, F_2, and the contact point and showing that all ellipses share a single bounding ellipse.

We further describe the loci of the centers, foci, and vertices of the family – circles and conchoids – and identify the limiting cases of maximal minor axis and vanishing eccentricity. The construction provides a concise geometric interpretation of the vis-viva relation and unites classical conic geometry with orbital dynamics.

4 The Vis-Viva Equation

The vis–viva relation (1) remains the cornerstone of orbital mechanics and is discussed in detail in modern treatments such as Murray and Dermott [9], Roy [11], Danby [4], and Vallado [12].

It states that

$$\mathrm{v}^2 = \mu\left(\frac{2}{\mathrm{r}} - \frac{1}{a}\right), \tag{1}$$

where

- v is the instantaneous orbital velocity of the moving body,
- r its current distance from the focus F_1 (the central mass),
- a the semimajor axis of the corresponding Kepler ellipse,
- $\mu = \mathrm{G}M$ the *gravitational parameter*,

and

$$\mathrm{G} = 6.67430 \times 10^{-11}\,\mathrm{m}^3\,\mathrm{kg}^{-1}\,\mathrm{s}^{-2}$$

denotes the universal gravitational constant, M the mass of the central attracting body.

Equation (1) expresses the conservation of total mechanical energy along a Keplerian orbit. The first term, $\frac{1}{2}\mathrm{v}^2$, represents the specific kinetic energy, whereas μ/r denotes the negative potential term. The relation applies equally to elliptical, parabolic, and hyperbolic trajectories, and reduces to the circular case when $\mathrm{r} = a$, yielding $\mathrm{v} = \sqrt{\mu/\mathrm{r}}$.

In the form of Eq. (1), one essentially determines the orbital speed v from the given semimajor axis a and the instantaneous distance r. It is noteworthy that the equation contains *no information* about the direction of the velocity vector $\vec{v}$; it merely provides its magnitude $\mathrm{v} = \|\vec{v}\|$.

Conversely, if the instantaneous orbital velocity v and the current distance r are known, the semimajor axis a of the corresponding Keplerian ellipse can be derived directly from Eq. (1):

$$\boxed{\frac{1}{a} = \frac{2}{\mathrm{r}} - \frac{\mathrm{v}^2}{\mu} \quad \Longleftrightarrow \quad a = \frac{1}{\dfrac{2}{\mathrm{r}} - \dfrac{\mathrm{v}^2}{\mu}}\,.} \tag{2}$$

This inverse form is widely used in orbital mechanics to compute the semimajor axis from position–velocity data at any given point of the trajectory.

From a *geometrical* point of view, Eq. (2) expresses that the orbital energy –, and thus the size of the ellipse – is completely determined by the *instantaneous* position and speed of the moving body. In the plane of motion, the direction of the velocity vector $\vec{v}$ is tangent to the ellipse at the current point, while its magnitude defines, through Eq. (1), the scale of the entire orbit. Consequently, the value of a derived from a single observation (r, v) uniquely determines the corresponding ellipse, up to the spatial orientation of its major axis.

A particularly important limiting case of Eq. (1) occurs when the semimajor axis a tends to infinity, corresponding to a *parabolic escape trajectory*. In this limit, the total mechanical energy approaches zero, and the orbital speed becomes the *escape velocity*

$$\boxed{\mathrm{v}_e = \sqrt{\frac{2\mu}{\mathrm{r}}}}\,. \tag{3}$$

Any higher velocity results in a hyperbolic orbit and permanent escape from the gravitational field of the central body. Conversely, for $\mathrm{v} < \mathrm{v}_e$ the motion remains bound, and Eq. (2) yields a finite semimajor axis a.

From a purely geometrical standpoint, the escape velocity marks the limiting case in which the semimajor axis a of the Kepler ellipse tends to infinity. As $a \to \infty$, the ellipse gradually opens, its curvature at the current point decreases, and the second focus recedes to infinity. The ellipse thus transforms smoothly into a *parabola* whose focus coincides with the central mass F_1 and whose directrix lies at an infinite distance.

In this limiting configuration, the moving body possesses just enough kinetic energy to reach infinity with zero residual speed – precisely the condition $\mathrm{v} = \mathrm{v}_e = \sqrt{2\mu/\mathrm{r}}$. Hence, the parabolic orbit forms the natural boundary between bound and unbound motion, connecting the family of Keplerian ellipses continuously to the branch of hyperbolic trajectories.

Remark 1 (Bound-Unbound Criterion) *In order to ensure that the curve κ_ψ represents a* closed Keplerian ellipse*, the orbital velocity* v *in the given point P must not exceed the* parabolic escape velocity. *Quantitatively, this means that the instantaneous velocity* v *may at most exceed the circular velocity* $\mathrm{v}_{\mathrm{circ}}$ *by a factor of* $\sqrt{2}$*:*

$$\mathrm{v} \le \sqrt{2}\,\mathrm{v}_{\mathrm{circ}} \quad \textit{with} \quad \mathrm{v}_{\mathrm{circ}} = \sqrt{\frac{\mu}{r}}.$$

If $\mathrm{v} = \sqrt{2}\,\mathrm{v}_{\mathrm{circ}}$*, the resulting orbit becomes parabolic* ($a \to \infty$)*; for* $\mathrm{v} > \sqrt{2}\,\mathrm{v}_{\mathrm{circ}}$*, it turns into a hyperbola. This* $\sqrt{2}$*-limit provides a simple geometric criterion for distinguishing bounded (elliptic) from unbounded (parabolic or hyperbolic) trajectories, and it holds universally for all central gravitational fields for all central gravitational fields (see [1, pp. 66–68]).*

In the present paper, however, we shall restrict our attention exclusively to *elliptical orbits*, leaving the parabolic and hyperbolic cases aside.

Remark 2 (Constant Period and Spatial Interpretation) *Since the semimajor axis a is identical for all members of the considered family of Keplerian ellipses, the orbital period T is the same for all of them as well, according to Kepler's third law,*

$$T = 2\pi\sqrt{\frac{a^3}{\mu}}.$$

Thus, all particles moving on these ellipses complete their revolution in equal time, even though their orbital shapes and instantaneous velocities differ.

Because the construction depends only on the line through F_1 and P, the same argument applies to any plane containing this line. Hence the family may be regarded as a three-dimensional system of identical orbits distributed over all planes passing through F_1P. In this sense, the model admits a natural spatial interpretation: Each ellipse represents the projection of an orbit lying in a different orbital plane but governed by the same gravitational parameter μ and the same total energy.

The time-evolution of the corresponding particles can be visualized by the accompanying sequence of frames shown in Fig. 2, and in the supplementary video available online ([5]).

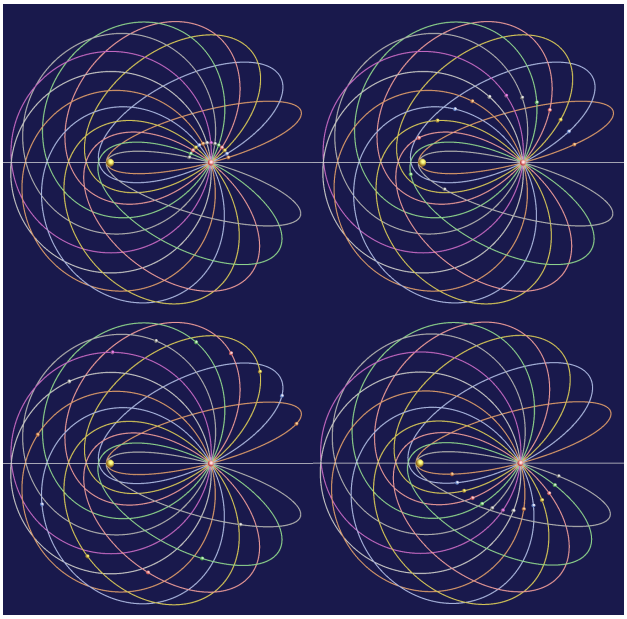

Figure 2: *Sequence of frames illustrating the motion of several particles along the family of Keplerian ellipses with identical semimajor axis a and focus F_1. Each ellipse corresponds to a different orientation of the tangent at P, but all orbits share the same period T and gravitational parameter μ, as illustrated in the supplementary video [5].*

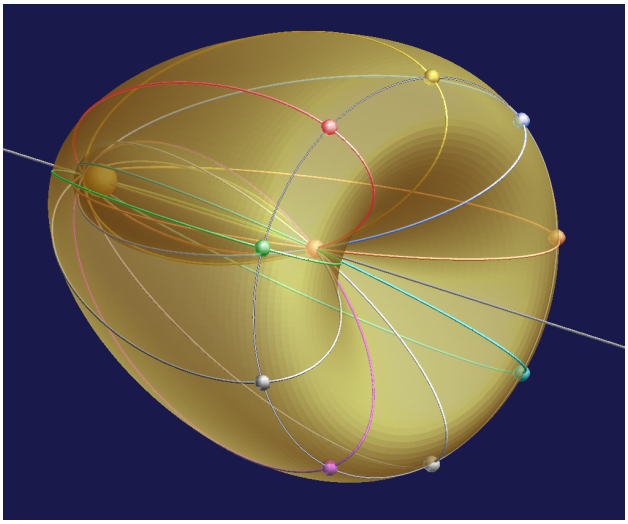

Figure 3: *Isoenergetic family of Keplerian trajectories launched with identical speed from the same point along all directions of a conical field of initial velocities. All orbits share the same semimajor axis a but differ in eccentricity and orientation. They return to the common starting point simultaneously after one complete revolution.*

Launching from the same point with identical speed along all directions of a cone of revolution whose axis is the orbital tangent yields an isoenergetic family of Keplerian ellipses with the same semimajor axis a but generally different eccentricities. All trajectories of this family have identical orbital periods, since the revolution time depends solely on the semimajor axis according to Kepler's third law. Consequently, although the eccentricities and spatial orientations of the orbits differ, all projectiles return to their common starting point simultaneously after one full revolution. The resulting configuration is illustrated in Fig. 3.

The time-evolution of this isoenergetic family is illustrated in Fig. 2, where all trajectories start simultaneously from the same point and return to it after one full revolution. An animated version of this figure, showing the continuous propagation of the orbits and the simultaneous rendezvous of the projectiles, is available as supplementary material online.

5 Geometric Construction

Having examined the physical foundation of Keplerian motion, we now turn to a purely *geometrical interpretation* of the same family of ellipses. Instead of deriving the orbital parameters from forces and energies, we shall describe the entire configuration in terms of *fixed points, distances, and loci*. This approach reveals several remarkable geometric properties – in particular, the existence of an *envelope ellipse* that is tangent to all Keplerian ellipses of a given family. For a comprehensive geometric treatment of conic sections and their focal properties, see [6].

6 Geometrical Construction

Let us begin with the question of how to construct an ellipse when one focus F_1, the total major axis length $2a$, and a point P at a fixed distance $d = |F_1P|$ are given, together with the tangent t at P, which forms an angle ψ with the reference axis $\overline{F_1P}$. The solution is remarkably simple.

Since an ellipse is the locus of all points whose distances to two fixed foci sum to the constant $2a$, and since the tangent at any point bisects the angle between the focal radii, we proceed as follows (Fig. 4):

Construction. Define a fixed counterpoint G on the ray F_1P such that $|F_1G| = 2a$. Reflect G about the tangent t through P; the reflection point is F_2,

$$F_2 = \mathrm{Ref}_t(G).$$

As the tangent direction ψ varies, G remains fixed while its mirror image F_2 moves along a circle f centered at P with

radius

$|PF_2| = 2a - d$.

This circle represents the *locus of all possible second foci* of the family of ellipses κ_ψ. The tangent t bisects the focal angle,

$\angle GPF_2 = 2\psi \Rightarrow \angle F_1PF_2 = \pi - 2\psi$.

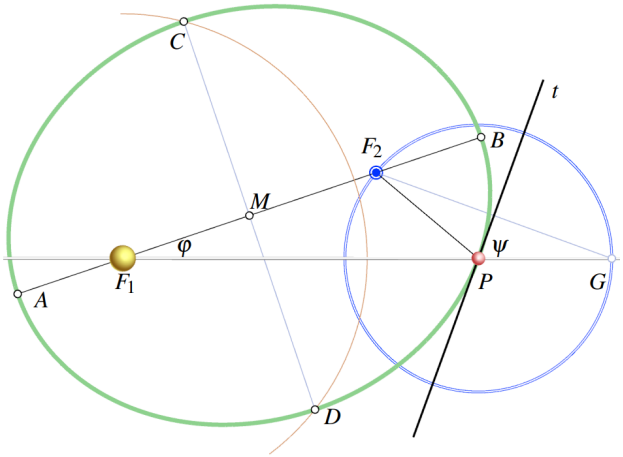

Figure 4: *Geometric construction of the ellipse κ_ψ from the given focus F_1, the tangent t at the point P with $|F_1P| = d$, and the total major axis $2a$. Reflect the line F_1P about t and mark on the reflected ray from P the segment of length $2a - d$ to obtain the second focus F_2. Equivalently, F_2 is the mirror image of the fixed point G on F_1P satisfying $|F_1G| = 2a$. The tangent t bisects the angle $\angle F_1PF_2 = \pi - 2\psi$. The construction fixes the center M, the vertices A, B, and the semiaxes $a, b(\psi)$.*

7 Three Circular Loci

Fix a focus F_1, a point P with $|F_1P| = d$, and a common semimajor axis a. For the one-parameter family $\{\kappa_\psi\}$ of Kepler ellipses through P we have:

1. **Locus of the second focus.** Evaluating the focal sum at $X = P$ gives $|PF_2| = 2a - d$. Hence the second focus F_2 runs on the circle

   f_2 : center P, radius $2a - d$.

2. **Locus of the ellipse centers.** Since the center M is the midpoint of F_1F_2, and F_2 moves on the circle around P, the midpoint $M = \frac{1}{2}(F_1 + F_2)$ describes a circle with half the radius and centered at the midpoint of F_1P. Writing Q for the midpoint of F_1P,

   m : center Q, radius $a - \frac{d}{2}$.

3. **Locus of the secondary vertices.** At the secondary vertices C, D the distances to the foci are equal by symmetry, and $|F_1C| + |F_2C| = 2a$ yields $|F_1C| = |F_2C| = a$ (likewise for D). Hence

   c : center F_1, radius a,

   i.e., all secondary vertices lie on the circle of radius a about F_1.

Figure 5 illustrates the configuration: The focus-locus f_2 (centered at P), the center-locus m (centered at the midpoint Q of F_1P), and the circle c carrying all secondary vertices C, D (centered at F_1).

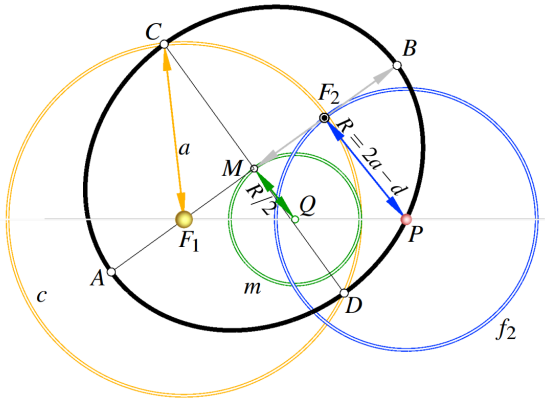

Figure 5: *Three circular loci for the family $\{\kappa_\psi\}$: The second focus F_2 moves on f_2 (center P, radius $2a - d$); the ellipse center M moves on m (center Q, the midpoint of F_1P, radius $a - \frac{d}{2}$); and the secondary vertices C, D lie on the circle c (center F_1, radius a).*

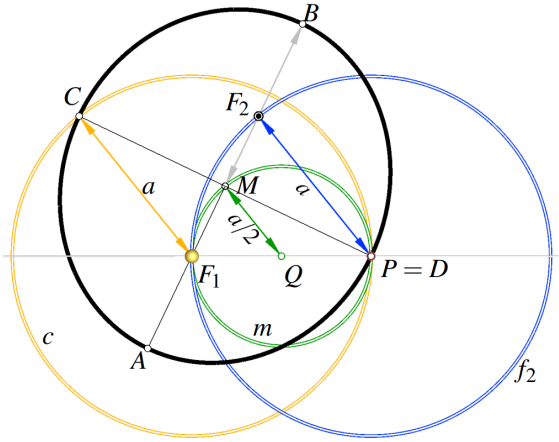

Figure 6: *Special case $a = d$: The focus locus f_2 (center P, radius a), the center locus m (center Q, radius $a/2$), and the circle c of minor vertices (center F_1, radius a).*

Remark 3 (Special case $a = d$) *In the special case $a = d$ the three circular loci simplify as follows: The second focus runs on f_2 with radius $|PF_2| = 2a - d = a$ (center P), the ellipse centers M run on m with radius $a - \frac{d}{2} = \frac{a}{2}$ (center Q, the midpoint of F_1P), and the minor vertices C, D lie on the circle c of radius a about F_1 (unchanged). The configuration is illustrated in Fig. 6.*
A particularly remarkable feature of this configuration is that the lower vertices *D of all ellipses coincide with the fixed point P.*

8 Focal distance and eccentricity

The midpoint M of the focal segment F_1F_2 is the center of κ_ψ, and satisfies

$$|F_1M| = |MF_2| = c_\psi,$$

which defines the *linear eccentricity*

$$c_\psi = \tfrac{1}{2}\sqrt{d^2 + (2a-d)^2 - 2d(2a-d)\cos(2\psi)}\,.$$

The corresponding (dimensionless) eccentricity is

$$e_\psi = \frac{c_\psi}{a}.$$

Equation of the ellipse. The ellipse κ_ψ has the polar equation (with origin at F_1, polar angle α measured from $\overline{F_1P}$):

$$r(\alpha) = \frac{a(1-e_\psi^2)}{1 + e_\psi\cos(\alpha - \varphi)},$$

where φ denotes the orientation of the major axis relative to $\overline{F_1P}$.

Remark 4 (Velocity Ratios at Pericenter and Apocenter) *For every Keplerian ellipse κ_ψ with semimajor axis a and eccentricity e_ψ, the instantaneous orbital velocity follows from the vis-viva relation*

$$\mathrm{v}^2 = \mu\left(\frac{2}{r} - \frac{1}{a}\right).$$

At the circular radius $r = a$ one obtains

$$\mathrm{v}_{\mathrm{circ}} = \sqrt{\frac{\mu}{a}}.$$

At pericenter and apocenter, where

$$r_{\mathrm{peri}} = a(1-e_\psi), \qquad r_{\mathrm{apo}} = a(1+e_\psi),$$

the corresponding velocities are

$$\mathrm{v}_{\mathrm{peri}} = \sqrt{\frac{\mu}{a}}\sqrt{\frac{1+e_\psi}{1-e_\psi}}, \qquad \mathrm{v}_{\mathrm{apo}} = \sqrt{\frac{\mu}{a}}\sqrt{\frac{1-e_\psi}{1+e_\psi}}.$$

Hence the ratios relative to the circular velocity are

$$\boxed{\frac{\mathrm{v}_{\mathrm{peri}}}{\mathrm{v}_{\mathrm{circ}}} = \sqrt{\frac{1+e_\psi}{1-e_\psi}}, \qquad \frac{\mathrm{v}_{\mathrm{apo}}}{\mathrm{v}_{\mathrm{circ}}} = \sqrt{\frac{1-e_\psi}{1+e_\psi}}.}$$

The pericentric velocity therefore exceeds the circular value, while the apocentric velocity falls below it. At the parabolic limit $e_\psi \to 1$ the pericentric velocity approaches $\sqrt{2}\,\mathrm{v}_{\mathrm{circ}}$, corresponding to the escape condition ([1, §2.5]).

Remark 5 (Special case $a = d$) *If the semimajor axis equals the focal distance to the given point, $a = d$, then the major axis of κ_ψ is aligned with the reflected ray through P, and the axis angle equals the tangent angle:*

$$\varphi = \psi.$$

In this case the eccentricity reduces to

$$e_\psi = \frac{c_\psi}{a} = \left|\sin\psi\right|,$$

and the vis–viva relations yield the pericentric and apocentric velocities, relative to the circular speed $\mathrm{v}_{\mathrm{circ}} = \sqrt{\mu/a}$:

$$\boxed{\frac{\mathrm{v}_{\mathrm{peri}}}{\mathrm{v}_{\mathrm{circ}}} = \sqrt{\frac{1+|\sin\psi|}{1-|\sin\psi|}}, \qquad \frac{\mathrm{v}_{\mathrm{apo}}}{\mathrm{v}_{\mathrm{circ}}} = \sqrt{\frac{1-|\sin\psi|}{1+|\sin\psi|}}}$$

(for ψ taken modulo π). At $\psi = 0$ one has $\mathrm{v}_{\mathrm{peri}} = \mathrm{v}_{\mathrm{apo}} = \mathrm{v}_{\mathrm{circ}}$ (circular case), while as $|\psi| \to \pi/2$ the apocentric velocity tends to 0 and $\mathrm{v}_{\mathrm{peri}} \to \sqrt{2}\,\mathrm{v}_{\mathrm{circ}}$ (parabolic limit).

Proof (vis–viva only). *From $\mathrm{v}^2 = \mu(2/r - 1/a)$, with $r_{\mathrm{peri,apo}} = a(1 \mp e_\psi)$ and $e_\psi = |\sin\psi|$, one obtains directly $\mathrm{v}_{\mathrm{peri}} = \mathrm{v}_{\mathrm{circ}}\sqrt{(1+e_\psi)/(1-e_\psi)}$ and $\mathrm{v}_{\mathrm{apo}} = \mathrm{v}_{\mathrm{circ}}\sqrt{(1-e_\psi)/(1+e_\psi)}$.*

Semiminor axis. From $b^2 = a^2 - c_\psi^2$ follows

$$b^2(\psi) = d\left(a - \frac{d}{2}\right) + \frac{d(2a-d)}{2}\cos(2\psi),$$

and thus,

$$b(\psi) = \cos\psi\sqrt{d(2a-d)}.$$

Hence the semiminor axis attains its maximum for $\psi = 0$, when the tangent is parallel to $\overline{F_1P}$:

$$b_{\max} = \sqrt{d(2a-d)}.$$

This value equals the geometric mean of the focal distances $d = |F_1P|$ and $(2a-d) = |PF_2|$. For $\psi = \frac{\pi}{2}$, the points F_1, P, and F_2 become collinear, the focal separation is maximal ($c_\psi = a$), and the ellipse degenerates into a line segment.

Summary. The family κ_ψ is completely determined by the parameters (a, d, ψ). The quantities φ, e_ψ, c_ψ, and $b(\psi)$ follow from the above relations. The fixed point G serves as a convenient geometric reference: All members of the family arise as mirror images of G with respect to their respective tangents $t(\psi)$.

9 The Envelope of the Family of Keplerian Ellipses

Let κ_ψ be one of the Kepler ellipses of the family. We mark on it a point H as the second intersection of the ellipse with the guiding ray PF_2. For this point, the sum of the focal distances is constant. Since

$$\begin{aligned} |F_1H| + |PH| &= \big\{\, |F_1H| + |F_2H| \,\big\} + |F_2P| \\ &= \big\{\, 2a \,\big\} + (2a - d) = 4a - d, \end{aligned}$$

the point H lies on an auxiliary ellipse h with foci F_1 and P and semimajor axis $2a - \frac{d}{2}$. At H, the tangents to κ_ψ and h coincide, because in both cases the tangent is the angle bisector of the same pair of guiding rays. Consequently, h touches every member of the family κ_ψ, and therefore, constitutes the *envelope* of all Keplerian ellipses of this type.

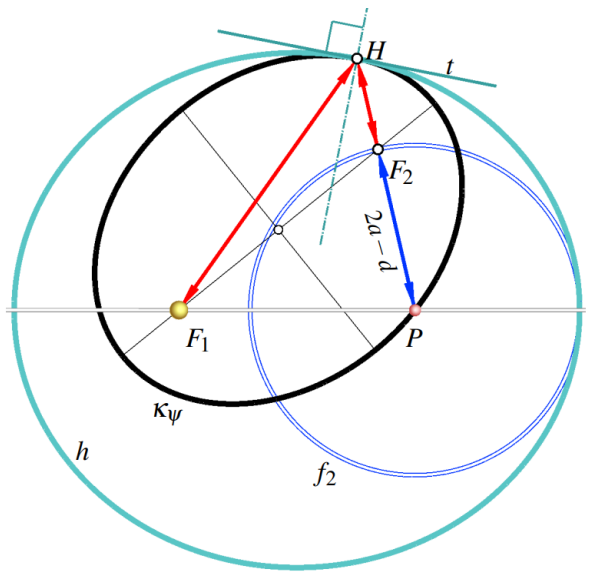

Figure 7: *Geometric proof of the envelope. For each tangent t through P, the reflection of the ray SP determines the second focus F_2. The intersection of the line PF_2 with the family's outer boundary defines the point H, which lies on the envelope ellipse h. The points P, F_2, and H are collinear.*

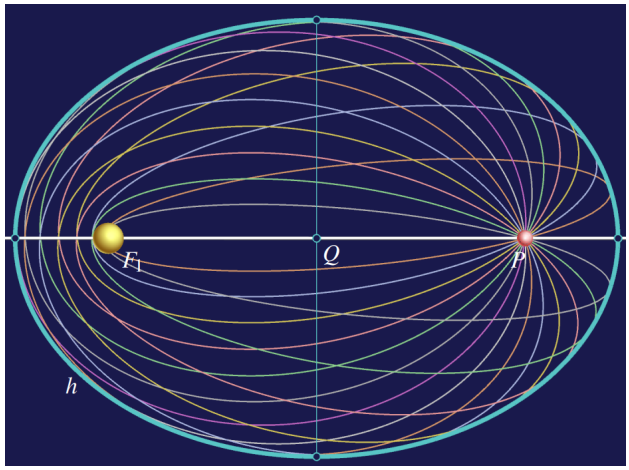

Figure 8: *The complete family of Kepler ellipses with fixed focus F_1 and identical speed at P. Each ellipse touches the envelope h (cyan curve). The envelope itself is an ellipse with semimajor axis $a_h = 2a - d$ and semiminor axis $b_h = \sqrt{(2a-d)d}$.*

The overall configuration is illustrated schematically in Fig. 7, showing the family of ellipses for different orientations of the tangent at P and their envelope h.

Moreover, the reflection of the point of contact H in the common tangent t always lies on the principal axis F_1P, at a distance of $4a - d$ from F_1.

Remark 6 (On intersections within the family) *Two distinct members κ_ψ and $\kappa_{\psi'}$ of the constant-speed family pass through P but have different tangents there (for $\psi \neq \psi'$), hence the intersection at P is transveral. By Bézout's theorem, two conics intersect with total multiplicity 4 in the complex projective plane; the remaining intersection multiplicities are accounted for by two common (complex) tangents through the fixed focus F_1 in the dual picture. Thus, neighbouring members typically meet only at P in the real plane.*

Spatial version. For each admissible tangential velocity at P, the corresponding Kepler ellipse κ_ψ is tangent to the envelope ellipse h with foci F_1 and P and semimajor axis $a_h = 2a - \frac{d}{2}$. If the entire configuration is rotated about the axis F_1P, the envelope h generates an *egg-shaped ellipsoid of revolution* whose focal points are F_1 and P.

As the velocity in P varies, the semimajor axis a changes according to the vis-viva relation $a = \frac{\mu r}{2\mu - r v^2}$, so that a ranges from 0 (for $v \to \infty$) up to $d\sqrt{2}$ at the parabolic limit. Hence all Keplerian ellipses passing through the fixed point P with any sub-parabolic velocity form a continuous one-parameter

family of *confocal egg-shaped ellipsoids of revolution* – as discussed in [10] – each touching its corresponding planar Kepler ellipse along the generator defined by the common tangent at P.

Remark 7 (The complete picture, a spatial arrangement of Keplerian ellipses) *Through the fixed point P there pass infinitely many tangents t, each characterized by its spatial orientation (two degrees of freedom) and by the magnitude of the velocity vector (one additional degree of freedom). Hence, the set of all Kepler ellipses passing through P forms a three-dimensional continuum: For every direction and speed in P there exists exactly one Keplerian orbit of the family.*

However, among these infinitely many ellipses, all those that differ only by a rigid motion (translation or rotation) are congruent. Thus, within this three-dimensional continuum, there exists a one-dimensional subfamily of congruent ellipses, leaving only a two-dimensional manifold of distinct shapes. Equivalently, if the semiaxes a and b are taken as parameters, the space of all geometrically different ellipses is two-dimensional, corresponding to the degrees of freedom of shape and eccentricity.

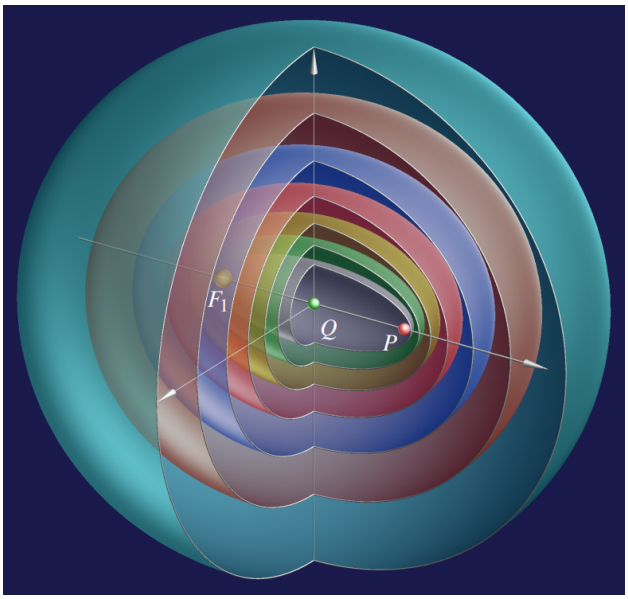

Figure 9: *Rotation of the envelope ellipse h about the axis F_1P generates an egg-shaped ellipsoid of revolution. The fixed points F_1 and P serve as common foci of all such ellipsoids, each corresponding to a Kepler ellipse κ_ψ of equal velocity in P. The colored layers illustrate the associated system of* confocal quadrics *sharing the same focal points F_1 and P. Each planar Kepler ellipse arises as a section through F_1, P, and its corresponding focus F_2.*

10 Loci of the Principal Vertices A and B

We return zu the planar version. Let m be the circle of ellipse centers with center C (the midpoint of F_1P) and radius $r_0 = a - \frac{d}{2}$. With F_1 as pole, let φ denote the polar direction. The ray from F_1 at angle φ meets m at distance

$$s(\varphi) = \tfrac{d}{2}\cos\varphi + \sqrt{r_0^2 - (\tfrac{d}{2}\sin\varphi)^2}\,.$$

The principal vertices are obtained by shifting $\pm a$ along this ray:

$$\boxed{r_A(\varphi) = s(\varphi) + a, \qquad r_B(\varphi) = |\,s(\varphi) - a\,|}\,.$$

Hence both loci are *conchoids of the circle m with pole F_1*.

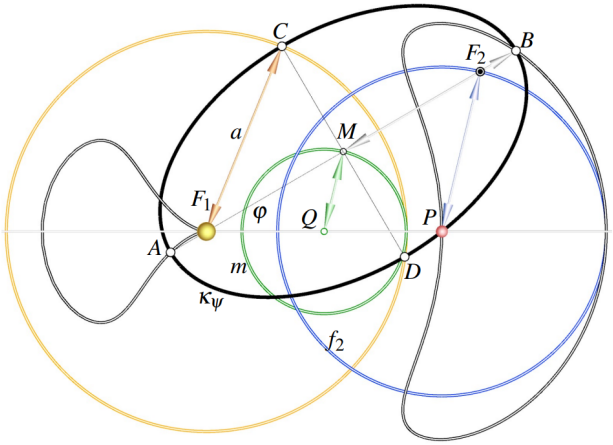

Figure 10: *General case: The loci of A (outer branch) and B (inner branch) are conchoids of the center circle m with pole F_1.*

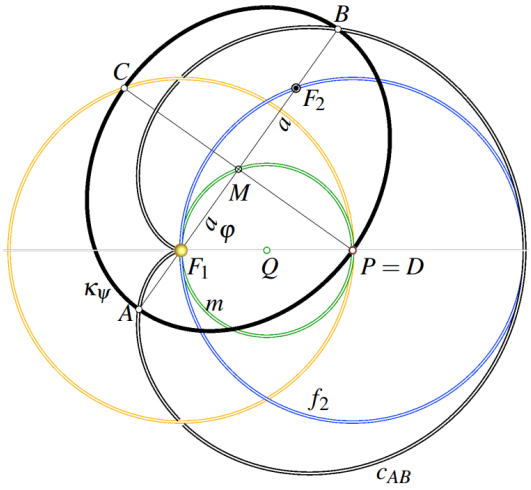

Figure 11: *Special case $a = d$: The conchoids degenerate into a cusped Pascal snail c_{AB}.*

Remark 8 (Identity of the two Pascal snails) *For the special case $a = d$, the loci of the two main vertices A and B of the ellipses κ_φ are given in polar coordinates by*

$$r_A(\varphi) = a(1+\cos\varphi), \qquad r_B(\varphi) = a(1-\cos\varphi).$$

Although these equations look different, they describe the same cusped Pascal snail *(a cardioid–type limaçon), merely rotated by π:*

$$r_B(\varphi+\pi) = a(1+\cos\varphi) = r_A(\varphi).$$

Hence the two vertex loci coincide geometrically, each covering the same curve twice with opposite orientation. The cusp corresponds to $\varphi = 0$, where A and B coincide at P, and the maximal distance $r = 2a$ occurs at $\varphi = \pi$.

The loci of the two main vertices A and B of all ellipses κ_φ (for the case $a = d$) form a single cusped Pascal snail *given in polar coordinates by $r = a(1+\cos\varphi)$. The cusp corresponds to $\varphi = 0$, where A and B coincide at P, and the maximal distance $r = 2a$ occurs at $\varphi = \pi$.*

In order to visualize the variation of the orbital velocity along this curve, we now plot the apocentric speed v_{apo} of the corresponding ellipses κ_φ above the cardioid. If the velocity is plotted with opposite sign for $-\frac{\pi}{2} < \varphi < +\frac{\pi}{2}$, the surface becomes continuous and differentiable at the parabolic limits. This orientation change reflects the natural reversal of motion along the cardioid when the orbit passes through its side point.

For a continuous, orientation preserving plot we use the signed apocentric speed

$$v^{\text{or}}_{\text{apo}}(\varphi) = s(\varphi)\, v_{\text{circ}} \sqrt{\frac{1-|\sin\varphi|}{1+|\sin\varphi|}}, \qquad s(\varphi) = -\operatorname{sgn}(\cos\varphi),$$

so that the sign flips at $\varphi = \pm\frac{\pi}{2}$.

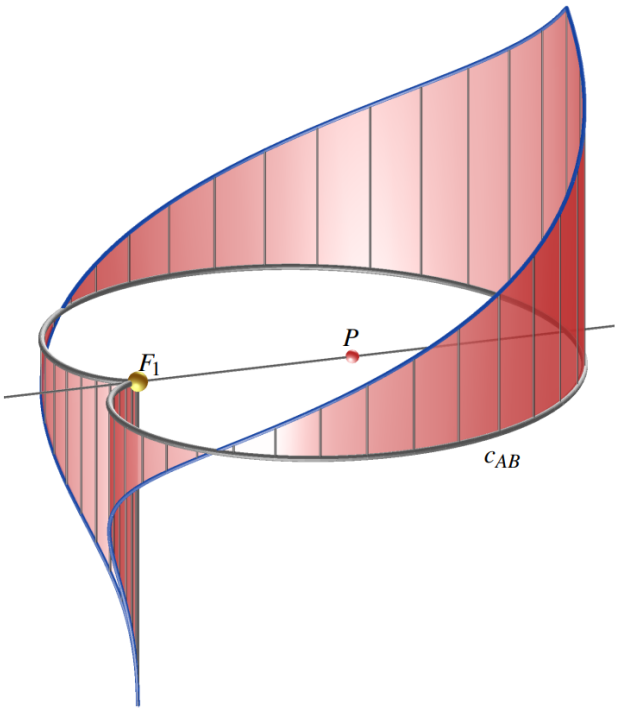

Figure 12: *Signed apocentric velocity over the cardioid $r = a(1+\cos\varphi)$. The black curve is the locus of apocentric vertices B (case $a = d$). The red ribbon shows $v^{\text{or}}_{\text{apo}}(\varphi)$, with the sign chosen via $s(\varphi) = -\operatorname{sgn}(\cos\varphi)$, yielding a smooth continuation through the parabolic limit $v_{\text{apo}} = 0$ at $\varphi = \pm\frac{\pi}{2}$.*

Conclusions and Future Work

The geometric constructions discussed above reveal a remarkable coherence between the analytic and envelope representations of the Kepler family. Starting from a purely planar setting, the reflection-based construction provides an intuitive bridge between the focal geometry of conic sections and their dynamical interpretation.

We have presented a purely geometric treatment of a remarkable family of Keplerian ellipses passing through a fixed point P with identical speed. By reflecting the ray F_1P in the tangent at P we located the second focus F_2 and established a simple proof that all such ellipses share a common bounding ellipse as their envelope. The semiaxes of this envelope can be expressed in closed form in terms of a and d.

In addition, we derived the loci of the centers, foci, and vertices of the entire family. The centers and minor vertices describe circles, whereas the principal vertices trace conchoids of the center circle, merging into a cusped Pascal snail in the special case $a = d$. These constructions demonstrate that classical geometry naturally reproduces the relations known from orbital mechanics.

From a physical point of view, the constant-speed family represents all possible bound orbits of equal total energy starting from P. Each member corresponds to a distinct initial direction, yet all share the same period according to Kepler's third law. The envelope thus provides a geometric visualization of the energy boundary in a central field.

A three-dimensional interpretation arises when the envelope ellipse h is rotated about the axis F_1P, generating an *egg-shaped ellipsoid of revolution*. The entire family of Kepler ellipses can therefore be embedded into a system of *confocal quadrics* sharing the same foci F_1 and P, providing a spatial counterpart to the planar focal construction (cf. Fig. 9).

Future work may extend this approach to inclined orbital planes and precessing ellipses, or explore analogous envelope constructions for hyperbolic and parabolic trajectories. The presented geometric framework also lends itself to educational and visual applications linking classical geometry with dynamical systems.

Beyond the purely geometric framework presented here, the same configuration may also be viewed in a dynamical context. Considering, for instance, the Jupiter system with a massless satellite (a "null moon" moving in the same orbital plane, the geometry of the present family arises as the limiting case of the barycentric two-body system when the satellite mass tends to zero. In this limit, the fixed focus F_1 represents the planet, and the moving focus F_2 corresponds to the barycentre of the combined system, thus providing a natural physical interpretation of the focal envelope. This observation may open a link between purely geometric envelopes and dynamical orbital models and will be explored in a forthcoming study.

References

[1] BATE, R.R., MUELLER, D.D., WHITE, J.E., *Fundamentals of Astrodynamics*. Dover Publications, New York, 1971.

[2] BUTIKOV, E.I., Families of Keplerian orbits. *Eur. J. Phys.* **24** (2003), 175–183, https://doi.org/10.1088/0143-0807/24/2/358

[3] BUTIKOV, E.I., The envelope of ballistic trajectories and elliptic orbits. *Eur. J. Phys.* **83** (2015), 952–958, https://doi.org/10.1119/1.4928176

[4] DANBY, J.M.A., *Fundamentals of Celestial Mechanics*. 2nd ed. Willmann–Bell, Richmond, VA, 1988.

[5] GLAESER, G., *Kepler Ellipses: Animated Supplementary Video*. University of Applied Arts Vienna, 2025, https://tethys.uni-ak.ac.at/kepler-ellipsen.mp4

[6] GLAESER, G., STACHEL, H., ODEHNAL, B., *The Universe of Conics*. 2nd ed., Springer Spektrum, Heidelberg, 2024, https://doi.org/10.1007/978-3-662-70306-9

[7] HECKMAN, G.J., Exercises on the Kepler ellipses through a fixed point in space, after Otto Laporte. *Indag. Math.* **36**(6) (2025), 1592–1599, https://doi.org/10.1016/j.indag.2025.02.004

[8] LAPORTE, O., On Kepler Ellipses Starting from a Point in Space. *Am. J. Phys* **38** (1970), 837–840, https://doi.org/10.1119/1.1976479

[9] MURRAY, C.D., DERMOTT, S.F., *Solar System Dynamics*. Cambridge University Press, Cambridge, 1999.

[10] ODEHNAL, B., STACHEL, H., GLAESER, G., *The Universe of Quadrics*. Springer-Verlag, Berlin, Heidelberg, 2020, https://doi.org/10.1007/978-3-662-61053-4

[11] ROY, A.E., *Orbital Motion*, 4th ed., Institute of Physics Publishing, Bristol and Philadelphia, 2005.

[12] VALLADO, D.A., *Fundamentals of Astrodynamics and Applications*, 4th ed. Microcosm Press, Hawthorne, CA, 2013.

Georg Glaeser
e-mail: georg.glaeser@uni-ak.ac.at

University of Applied Arts Vienna
Oskar-Kokoschka-Platz 2, A-1010 Vienna, Austria